Progress In Electromagnetics Research, PIER 62, 193–201, 2006

NONLINEAR INVERSION OF MULTI-FREQUENCY MICROWAVE FRESNEL DATA USING THE MULTIPLICATIVE REGULARIZED CONTRAST SOURCE INVERSION

A. Abubakar and T. M. Habashy

Schlumberger-Doll Research, USA

P. M. van den Berg

Delft University of Technology, The Netherlands

Abstract—This paper presents the results of profile inversion of multi-frequency electromagnetic scattered field data, measured by the Institute Fresnel, Marseille, France, from cylindrical objects, both for TM and TE illuminations. The reconstructions are obtained by applying the Multiplicative Regularized Contrast Source Inversion (MR-CSI) method. The results show that the MR-CSI method successfully performs 'blind' inversion of a wide class of scattered field data. Further, we also show that by inverting both TM and TE data simultaneously, a more accurate reconstructed image can be obtained.

1. INTRODUCTION

We discuss the performance of the Contrast Source Inversion (CSI) method [1, 2], enhanced with a Multiplicative Regularization technique (MR-CSI) [3]. The MR-CSI method has been applied to invert the first set of data measured by the Institut Fresnel, Marseille, France [4]. The inversion results obtained using the MR-CSI method from these first Fresnel data sets were presented in [5]. Following these experiments, the MR-CSI method has been improved by the introduction of the so-called weighted L_2-norm regularizer, see [6]. The inversion results of the first Fresnel data set using the MR-CSI method with weighted L_2-norm regularizer can be found in [7].

With this version of the MR-CSI method we demonstrate the reconstructions from the second set of data measured by the Institut Fresnel. We carry out a 'blind' inversion of these data sets without

explicitly taking into consideration any *a priori* information regarding the type of objects (either dielectric or metallic) to be reconstructed. In all cases we reconstruct both the permittivity and the conductivity of the unknown objects. The only *a priori* information which is used in the inversion is the positivity constraint on both permittivity and conductivity. The inversion results show that the MR-CSI method seems to handle the experimental field data very well. Furthermore we will show that by inverting both TM and TE data simultaneously we are able to arrive at more accurate reconstructed images.

2. METHODOLOGY

The Institute Fresnel experimental setup consists of a transmitting and a receiving antennas, both of which are double-ridged horn antennas. The antennas are moved on a circular rail around the object(s). The objects are elongated in the direction perpendicular to the plane in which the antennas are rotated (i. e., the plane of measurement), that a two-dimensional (2D) model is appropriate. In the plane of illumination, we choose a 2D rectangular test domain D containing the object(s). The transmitting antenna illuminates the objects from different locations distributed equidistantly around the object. We use the subscript j to denote the measured frequency and the subscript s to denote the dependence on the transmitter position. The receiving antenna measures the total field and the incident field from a number of different locations distributed equidistantly around the object. The scattered field, which is needed in the inversion, can then be found by subtracting the incident field from the total field.

The experimental data are collected at a number of frequencies with time factor $\exp(-\mathrm{i}\omega_j t)$ where $\mathrm{i}^2 = -1$, ω_j is the radial frequency and t is time. We introduce the vectors $\boldsymbol{p}$ and $\boldsymbol{q}$ as the spatial positions in 2D. We use the Maxwell model for the constitutive parameters of the object. Hence the contrast function for each frequency is defined as follows:

$$\chi_j(\boldsymbol{q}) = \frac{\varepsilon(\boldsymbol{q}) - \varepsilon_0}{\varepsilon_0} + \mathrm{i}\frac{\sigma(\boldsymbol{q})}{\omega_j \varepsilon_0}, \tag{1}$$

where ε and σ denote the permittivity and conductivity, which are frequency independent. The symbol ε_0 denotes the permittivity in vacuum. Since ε and σ are frequency independent, it is obvious that in the inversion we need only to invert for one value of the contrast function. Let χ_1 be the contrast function value at the angular frequency ω_1, then the other values of the contrast as a function of

frequency can be calculated through:

$$\chi_j(\boldsymbol{q}) = \mathrm{Re}\left[\chi_1(\boldsymbol{q})\right] + \mathrm{i}\frac{\omega_1}{\omega_j}\mathrm{Im}\left[\chi_1(\boldsymbol{q})\right]. \tag{2}$$

Since all the objects lie inside a test domain D, the contrast function is therefore non-zero inside D and zero elsewhere.

In the *TM-case* where the non-zero component of the electric field is the only one parallel to the cylindrical objects, we deal with a scalar wave field problem. The domain integral representation for the scattered field as a function of the total field $u_{s,j}$ and the contrast χ_j is given by

$$u_{s,j}^{\mathrm{sct}}(\boldsymbol{p}) = K_j^{\mathrm{TM}}[\chi_j u_{s,j}] = k_{0,j}^2 \int_D g_j(\boldsymbol{p},\boldsymbol{q})\chi_j(\boldsymbol{q})u_{s,j}(\boldsymbol{q})\mathrm{dv}(\boldsymbol{q}), \quad \boldsymbol{p} \in S, \tag{3}$$

where $k_{0,j} = \omega_j\sqrt{\varepsilon_0\mu_0}$ is the wave number in free-space and S is the data domain where the transmitter and receiver are located. The scalar homogeneous Green function is given by

$$g_j(\boldsymbol{p},\boldsymbol{q}) = \frac{\mathrm{i}}{4}H_0^{(1)}(k_{0,j}|\boldsymbol{p}-\boldsymbol{q}|), \tag{4}$$

where $H_0^{(1)}$ denotes the first kind Hankel function of zero order.

In the *TE-case*, the field quantities are two-components vectors representing the electric field components in the transversal plane of the cylindrical objects. The domain integral representation for the scattered field vector as a function of the total field $\boldsymbol{u}_{s,j}$ and the contrast χ_j is given by

$$\begin{aligned} \boldsymbol{u}_{s,j}^{\mathrm{sct}}(\boldsymbol{p}) &= K_j^{\mathrm{TE}}[\chi_j \boldsymbol{u}_{s,j}] \\ &= (k_{0,j}^2 + \nabla\nabla\cdot)\int_D g_j(\boldsymbol{p},\boldsymbol{q})\chi_j(\boldsymbol{q})\boldsymbol{u}_{s,j}(\boldsymbol{q})\mathrm{dv}(\boldsymbol{q}), \quad \boldsymbol{p} \in S, \end{aligned} \tag{5}$$

where ∇ is the spatial differentiation operator with respect to $\boldsymbol{p}$.

The TM and TE total field, and the contrast inside the test domain D satisfy the following integral equation:

$$\begin{aligned} u_{s,j}^{\mathrm{inc}}(\boldsymbol{p}) &= u_{s,j}(\boldsymbol{p}) - K_j^{\mathrm{TM}}[\chi_{j,n}u_{s,j,n}], \\ \boldsymbol{u}_{s,j}^{\mathrm{inc}}(\boldsymbol{p}) &= \boldsymbol{u}_{s,j}(\boldsymbol{p}) - K_j^{\mathrm{TE}}[\chi_{j,n}\boldsymbol{u}_{s,j,n}], \quad \boldsymbol{p} \in D \end{aligned} \tag{6}$$

where the operators $K_j^{\mathrm{TM}}[\chi_j u_{s,j}]$ and $K_j^{\mathrm{TE}}[\chi_j \boldsymbol{u}_{s,j}]$ are defined in (3) and (5), for the TM-case and TE-case respectively. Equations (3), (5) and (6) are the basic equations for developing any inversion algorithm

based on the integral equation formulation. The goal of solving the inverse scattering problem can be formulated as follows: Solve (3) or (5) to obtain the contrast χ_1 on D from the knowledge of the scattered field $u^{\rm sct}_{s,j}$ on S and the incident field $u^{\rm inc}_{s,j}$ on D subject to the necessary condition that the total field $u_{s,j}$ on D and the contrast χ_1 on D satisfy the integral equation in (6).

We consider the inverse scattering problem as an optimization problem where, in each iteration n, we update the contrast sources $w_{s,j,n} = \chi_j u_{s,j,n}$ and the contrast $\chi_{j,n}$ alternatingly, by minimization of the cost function. For the TM inversion the cost function is given by

$$F_n(\chi_{1,n}, w_{s,j,n}) = \left[\frac{\sum_{s,j} \left\| u^{\rm sct}_{s,j} - K^{\rm TM}_j[w_{s,j,n}] \right\|^2_S}{\sum_{s,j} \left\| u^{\rm sct}_{s,j} \right\|^2_S} + \frac{\sum_{s,j} \left\| w_{s,j,n} - \chi_{j,n} u_{s,j,n} \right\|^2_D}{\sum_{s,j} \left\| \chi_{j,n-1} u^{\rm inc}_{s,j} \right\|^2_D} \right] \cdot \int_D \frac{|\chi_{1,n}(\boldsymbol{p})|^2 + \delta_n^2}{|\chi_{1,n-1}(\boldsymbol{p})|^2 + \delta_n^2} {\rm dv}(\boldsymbol{p}), \tag{7}$$

where

$$u_{s,j,n} = u^{\rm inc}_{s,j} + K^{\rm TM}_j[w_{s,j,n}], \quad \delta_n^2 = \frac{1}{\Delta^2} \frac{\sum_{s,j} \left\| w_{s,j,n-1} - \chi_{j,n-1} u_{s,j,n-1} \right\|^2_D}{\sum_{s,j} \left\| \chi_{j,n-1} u^{\rm inc}_{s,j} \right\|^2_D} \tag{8}$$

and $\| \cdot \|^2_S$ and $\| \cdot \|^2_D$ denote the L_2-norm on the data domain S and the object domain D, respectively. The symbol Δ denotes the mesh size of the discretization grid. In this CSI method, we use the back-propagation step to arrive at initial estimates for the contrast sources and the contrast. After the initial step, in each iteration the contrast sources and the contrast are updated alternatingly each by using one conjugate gradient step. The optimization process may be terminated if one of the following stopping conditions is satisfied:

- The difference between the normalized data error F_n at two successive iterates, n-th and $(n-1)$-th, is within a prescribed error quantity (it set to be 10^{-5}).
- The total number of iterations exceeds a prescribed maximum $N_{\max} = 512$.

The *a priori* information that the permittivity and the conductivity are positive are implemented by enforcing the negative value to zero

after each iteration. This simple procedure is employed in all of the inversion runs. Details of this so-called MR-CSI method for multi-frequency problem can be found in [5]. However the procedure to update the contrast function is replaced by the improved version in [7]. For the TE inversion the cost function in (7) is replaced by

$$F_n(\chi_{1,n}, \boldsymbol{w}_{s,j,n}) = \left[\frac{\sum_{s,j} \left\| \boldsymbol{u}_{s,j}^{\mathrm{sct}} - K_j^{\mathrm{TE}}[\boldsymbol{w}_{s,j,n}] \right\|_S^2}{\sum_{s,j} \left\| \boldsymbol{u}_{s,j}^{\mathrm{sct}} \right\|_S^2} + \frac{\sum_{s,j} \left\| \boldsymbol{w}_{s,j,n} - \chi_{j,n} \boldsymbol{u}_{s,j,n} \right\|_D^2}{\sum_{s,j} \left\| \chi_{j,n-1} \boldsymbol{u}_{s,j}^{\mathrm{inc}} \right\|_D^2} \right] \cdot \int_D \frac{|\chi_{1,n}(\boldsymbol{p})|^2 + \delta_n^2}{|\chi_{1,n-1}(\boldsymbol{p})|^2 + \delta_n^2} \mathrm{dv}(\boldsymbol{p}), \tag{9}$$

where

$$\boldsymbol{u}_{s,j,n} = \boldsymbol{u}_{s,j}^{inc} + K_j^{\mathrm{TE}}[\boldsymbol{w}_{s,j,n}]. \tag{10}$$

Further, for joint TM and TE data inversion, the cost function to be minimized is given by

$$\begin{aligned} F_n(\chi_{1,n}, w_{s,j,n}, \boldsymbol{w}_{s,j,n}) = & \\ & \left[\frac{\sum_{s,j} \left\| u_{s,j}^{\mathrm{sct}} - K_j^{\mathrm{TM}}[w_{s,j,n}] \right\|_S^2}{\sum_{s,j} \left\| u_{s,j}^{\mathrm{sct}} \right\|_S^2} + \frac{\sum_{s,j} \left\| w_{s,j,n} - \chi_{j,n} u_{s,j,n} \right\|_D^2}{\sum_{s,j} \left\| \chi_{j,n-1} u_{s,j}^{inc} \right\|_D^2} \right. \\ & \left. + \frac{\sum_{s,j} \left\| \boldsymbol{u}_{s,j}^{\mathrm{sct}} - K_j^{\mathrm{TE}}[\boldsymbol{w}_{s,j,n}] \right\|_S^2}{\sum_{s,j} \left\| \boldsymbol{u}_{s,j}^{\mathrm{sct}} \right\|_S^2} + \frac{\sum_{s,j} \left\| \boldsymbol{w}_{s,j,n} - \chi_{j,n} \boldsymbol{u}_{s,j,n} \right\|_D^2}{\sum_{s,j} \left\| \chi_{j,n-1} \boldsymbol{u}_{s,j}^{inc} \right\|_D^2} \right] \\ & \cdot \int_D \frac{|\chi_{1,n}(\boldsymbol{p})|^2 + \delta_n^2}{|\chi_{1,n-1}(\boldsymbol{p})|^2 + \delta_n^2} \mathrm{dv}(\boldsymbol{p}). \end{aligned} \tag{11}$$

3. NUMERICAL RESULTS

In this paper we only show the inversion results of the data sets FoamMetExtTM.exp and FoamMetExtTE.exp. These data sets FoamMetExtTM.exp and FoamMetExtTE.exp are obtained by measuring a configuration as shown in Fig. 1. This configuration consists of one circular dielectric cylinder with a relative permittivity value of $\varepsilon_r = 1.45$ with a diameter of 80 mm and one metallic

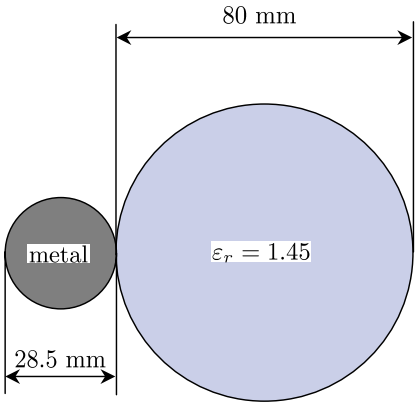

Figure 1. The configuration used to obtain the data sets FoamMetExtTM.exp and FoamMetExtTE.exp.

cylinder with a diameter of 28.5 mm. In the experiment, there are 18 transmitters distributed uniformly on a circle with a radius of 1.67 m from the center of the experimental setup. For each transmitter the data are measured using 241 receivers located on a circle with a radius of 1.67 m. The data are collected at 17 frequencies in the range of 2–18 GHz. In the experimental setup the fields are generated and received by horn antennas. However as we previously argued, the problem is predominantly 2D. Hence both receivers and transmitters are approximated as line receivers and line transmitters. Therefore, we carry out the calibration procedure outlined in [5].

In the inversion we take a test domain D of 16.775 cm by 16.775 cm. The test domain D is discretized into 122 by 122 rectangular subdomains. The side length of each subdomain is 0.1375 cm. The wavelength at 18 GHz is 1.67 cm, hence the width and height of the test domain D is 10 time the wavelength in vacuum. The data for different frequencies are inverted simultaneously. However, in the figures we plot the complex contrast function χ_1 only. This is the complex contrast at the lowest frequency.

The reconstructed images from the TM and TE data sets are shown in Figs. 2(a) and (b). The left plots give the distribution of the real part of the reconstructed contrast function and while the right plots give the distribution of the imaginary part of the reconstructed contrast function. The inversion results from TM data set (see Fig. 2(a)) show that the metallic cylinder is retrieved with real and imaginary parts having the same order of magnitude. These inversion results also show that there is an ambiguity in the inversion.

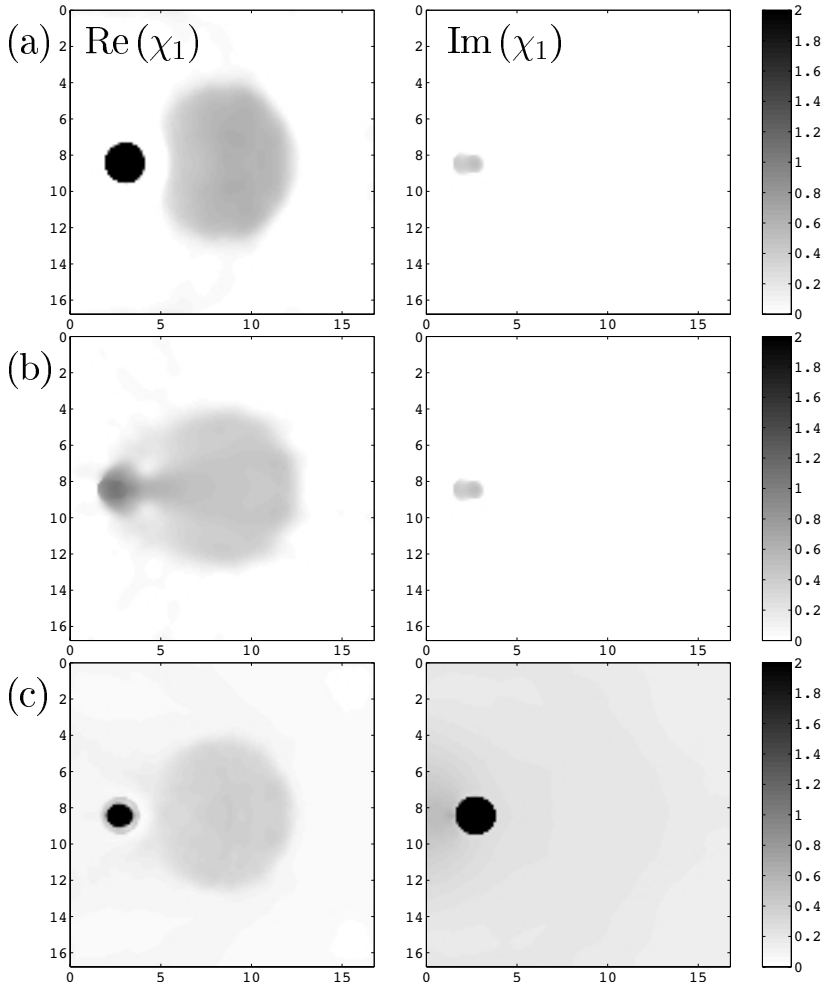

Figure 2. Reconstruction of the configuration with two disjoint cylinders, a dielectric one and a metallic one, for TM data polarization (data set: FoamMetExtTM.exp) (a) and TE data polarization (data set: FoamMetExtTE.exp) (b); and for joint inversion of both TM and TE data polarizations (c).

In principle, when carrying out the inversion of a perfectly conducting cylinder one can only reconstruct uniquely the boundary of the object. Inside the metal object the contrast sources are invisible, with the consequence that any contrast inside the object may be arbitrarily arrived at. The small circular object with a large permittivity value

appearing in the image of $\mathrm{Re}(\chi_1)$ is obviously an artifact of the inversion algorithm. However since the reconstructed circular object in $\mathrm{Re}(\chi_1)$ lies completely inside the circular cylinder in $\mathrm{Im}(\chi_1)$, one can conclude that we are dealing with a metallic object. On the other hand, the imaginary parts of the contrast of the TE inversion do not exhibit any significant features (see Fig. 2(b)). However the shape of the large dielectric cylinder is better reconstructed using the TE inversion than the one using the TM inversion.

Next we invert both the TM and TE data simultaneously. The results of this joint inversion are given in Fig. 2(c). By inverting both TM and TE data simultaneously we obtain an improved reconstructed image of the large dielectric cylinder. Furthermore the small artifact in the image of $\mathrm{Re}(\chi_1)$ is obviously lied completely inside the circular cylinder in $\mathrm{Im}(\chi_1)$. Hence, we can conclude that by inverting both the TM and TE data simultaneously we can obtain more accurate reconstructed images than by inverting the TM and TE data sets separately.

4. CONCLUSIONS

In view of the present results and our crude approximation of the transmitting and receiving antennas, the Multiplicative Regularized Contrast Source Inversion method seems to be very robust and is capable of 'blindly' handling a wide class of inverse scattering problems. Finally we note that by inverting both TM- and TE-data simultaneously, we can obtain more accurate reconstructed images.

ACKNOWLEDGMENT

The authors wish to thank Dr. M. Saillard and Dr. K. Belkebir for providing their second set of experimental data as an objective test of our inversion algorithm.

REFERENCES

1. Habashy, T. M., M. L. Oristaglio, and A. T. de Hoop, "Simultaneous nonlinear reconstruction of two-dimensional permittivity and conductivity," *Radio Science*, Vol. 29, 1101–1118, 1994.
2. Van den Berg, P. M. and R. E. Kleinman, "A contrast source inversion method," *Inverse Problems*, Vol. 13, 1607–1620, 1997.
3. Van den Berg, P. M., A. L. van Broekhoven, and A. Abubakar,

"Extended contrast source inversion," *Inverse Problems*, Vol. 15, 1325–1344, 1999.

4. Belkebir, K. and M. Saillard, "Guest editors' introduction, special section: testing inversion algorithms against experimental data," *Inverse Problems*, Vol. 17, 1565–1571, 2001.
5. Bloemenkamp, R. F., A. Abubakar, and P. M. van den Berg, "Inversion of experimental multi-frequency data using the contrast source inversion method," *Inverse Problems*, Vol. 17, 1611–1622, 2001.
6. Abubakar, A., P. M. van den Berg, and J. J. Mallorqui, "Imaging of biomedical data using a multiplicative regularized contrast source inversion method," *IEEE Transactions on Microwave Theory and Techniques*, Vol. 50, 1761–1771, 2002.
7. Van den Berg, P. M., A. Abubakar, and J. T. Fokkema, "Multiplicative regularization for contrast profile inversion," *Radio Science*, Vol. 38, 23.1–10, 2003.